On the Dynamics of Mobilization in Swelling–Dissolving Polymeric Systems†

I. Devotta, V. Premnath, M. V. Badiger, P. R. Rajamohanan, S. Ganapathy, and R. A. Mashelkar*

National Chemical Laboratory, Pune 411 008, India

Received December 23, 1992; Revised Manuscript Received September 30, 1993●

ABSTRACT: The dynamics of the swelling–dissolution process in a rubbery polymer has been probed at a microscopic level for the first time by doing *in situ* NMR measurements. Some preliminary experiments on swelling–dissolution of polyisoprene have been performed. The appearance of an intermediate plateau in the mobility vs time plot in this system is highly suggestive of "pseudoequilibrium" swelling, which persists for a surprisingly long time before any substantial dissolution can take place. Based on these microscopic observations, a mathematical model for the swelling–dissolution process has been developed which treats the swelling process and the dissolution process as distinct decoupled processes. "Disengagement" of polymer chains at the interface due to the hydrodynamic forces on the polymer chains dangling into the liquid has been postulated to be responsible for the increased dissolution rates under shearing conditions. The simple model developed is able to correctly predict the existence of the plateau under stagnant conditions as well as the disappearance of the plateau in a hydrodynamic field.

Introduction

When a solid polymer is brought in contact with a solvent, a stress field is created by the penetration of the solvent into the polymer matrix, resulting in swelling and, in some cases, complete dissolution of the polymer in the solvent. Macroscopic issues connected with the swelling and dissolution of glassy and rubbery polymers have been addressed for some time now. Invariably, measurements of the rate of penetration of the glass–gel front, thickness of the swollen polymer, and the concentration of the polymer in the medium are made.[1] Techniques such as refractometry, critical angle microscopy, interferometry, ellipsometry, etc. have been exploited to measure the thickness of the dissolving polymer films.

Apart from the study of the macroscopic manifestations, it is important to understand the dynamic events that take place at a molecular level. Such events have been probed by using many techniques such as small-angle neutron scattering, dynamic light scattering, nuclear magnetic resonance spectroscopy, etc.[2-4] However, these studies have been done under equilibrium conditions and the dynamics of events has been rarely probed[5] through such techniques.

In this paper, the dynamic events that take place at a microscopic level during the internal mobilization in a swelling–dissolving polymer will be examined by using solid-state nuclear magnetic resonance spectroscopy (NMR). NMR interactions being local in nature, the microscopic dynamic response can be sensed by the changes in segmental mobility by solvent imbibition. The response is sensed through the spectral and relaxation parameters of the chosen nucleus. Unlike the previously reported spectral characterization by the NMR technique in equilibrium swollen systems,[6-10] we will carry out dynamic measurements so that the process of polymer swelling and dissolution can be monitored temporally. Dynamic line width data obtained from such experiments will be interpreted in terms of the basic physical processes controlling the change of the internal mobility of the polymer chain, which essentially arise due to the swelling of the polymer matrix and the subsequent dissolution due to disengagement of the polymer chain from the surface of the polymer. A preliminary mathematical model will be developed, which will relate the internal mobility of the polymer chains to the polymer volume fraction. The new insights gained because of the experimental findings presented in this work will be highlighted at the end.

NMR Technique for the Study of Dynamics of Mobilization. We will first show that simple proton NMR spectral measurements can be conveniently carried out by using the magnetically abundant ^{1}H nucleus. The temporal response is also carried out *in situ*, and this can be shown to be related to the microscopic behavior in the chain in response to the macroscopic perturbation (by solvent) through the enhanced molecular mobilities that tend to narrow the otherwise broad proton resonance line. We have chosen to use ^{1}H spectral measurements because of the increased sensitivity and the resolution with which NMR resonance can be detected. *In situ* time-averaging effects are minimal, since signal averaging in the time domain can be accomplished within a short time (of the order of a minute).

We will use the change of proton line width as a direct measure of the local mobility in a swelling–dissolving system, since this change emanates from a spatial averaging of local spin interactions by polymer motions. In the present case, the dominant line width contributor is the ^{1}H–^{1}H homonuclear dipolar interactions between various interacting protons in the polymer repeat units. This includes both the intramolecular (within the monomer) and intermolecular (adjacent units) dipolar interactions. The line broadening is governed by the powder averaged second moment of the proton line, given by[11]

$$M_2 = \frac{3}{5}\gamma^4\hbar^2 I(I+1)\sum_{j>k}\frac{1}{r_{jk}^{\ 6}} \qquad (1)$$

where I is the spin number, $\hbar$ is Planck's constant, γ is the magnetogyric ratio, and r_{jk} denotes the internuclear distance between the jth and kth proton in the polymer, summed over all interacting pairs. The resulting line is

---

* To whom all correspondence should be addressed. Also at Jawaharlal Nehru Centre for Advanced Scientific Research, Bangalore.

† NCL communication no. 5660.

● Abstract published in *Advance ACS Abstracts*, December 1, 1993.

0024-9297/94/2227-0532$04.50/0

essentially a Gaussian with a line width $\Delta\nu = 2.36\ M_2^{1/2}$. Such interactions in a rigid array of ^{1}H dipoles would normally yield $\langle M_2 \rangle = 2 \times 10^{-5}$ s^{-2} (or $\Delta\nu = 45$ kHz). It is important to note here that the total second moment of the proton resonance line is invariant to lattice motions, whereas the observable part of M_2, measured experimentally, is not.[11] However, when molecular motions become more rapid, the various pairwise interactions get spatially averaged to yield reduced M_2 or, equivalently, reduced $\Delta\nu$. The extent of averaging, of course, depends on the details of the motional processes involved.

In a rubbery material (such as polyisoprene used in this work), the glass transition temperature is typically of the order of −50 °C. Therefore at temperatures well above the glass transition temperature, both the backbone and the side chain motions take place. They render considerable motional averaging of the associated ^{1}H–^{1}H interactions, thus causing a reduction in line width from the rigid lattice value. This is also the limiting line width one would observe at ambient temperature in the rubbery system before interaction with the solvent. As the solvent penetration into the polymer matrix takes place, the process of enhancement in local segmental mobility begins. At a microscopic level, the increase in the local free volume leads to a greater degree of movement of the various functional groups. As the degree of swelling increases, there is less hindrance to the process of local mobilization, and the motional correlation time decreases.

In rigid or semirigid solids, it is customary to relate the proton line width to the spin–spin relaxation time (T_2). When ^{1}H–^{1}H homonuclear dipolar interactions dominate, the observed proton line is lifetime broadened by the homogeneous nature of the dipolar Hamiltonian.[12] In a tightly spin-coupled proton system there is rapid "spin diffusion", the overall rate of which determines the spin–spin relaxation time T_2. The line width of the polymer proton line is exclusively determined by this T_2 mechanism. In rigid polymers, T_2 is typically of the order of 7–10 μs, resulting in a proton line width of 30–50 kHz. The solvent penetration into the polymer matrix attenuates the dipolar interaction between proton spins and weakens the spin diffusion process. Consequently, there is an increase in T_2 or a reduction in the line width, taking place progressively through some subtle but understandable mechanisms. When the solvent penetration is high, as in the case of an equilibrium swollen polymer, the spin diffusion is considerably inhibited, if not completely eliminated. Evidence for such processes was clearly demonstrated by us[14] and others[15,16] in a number of polymeric gels, where T_2 was found to increase drastically. Finally, in a polymer, where both swelling and dissolution processes occur at comparable rates, the motion of the polymer molecules in the solvent medium as well as that in the swollen state contributes to the observed line width. Separation of these biphasic components from the observed resonance line would not be possible when the component line widths are closer in value. However, when the dissolution occurs to a large extent, the contribution of the polymer molecules in the solvent to the measured line width will be significantly larger.

A simple BPP[17] treatment relates the experimentally determined line width to the motional correlation time τ_c, by

$$\frac{1}{T_2} = \frac{3}{40}\gamma^4\hbar^2\sum_k r_{jk}^{-6}\{6J(0) + 10J(\omega_0) + 4J(2\omega_0)\} \qquad (2)$$

where the different symbols have their usual meanings and the summation is over various pairwise interactions. In the extreme narrowing limit ($\omega_0\tau_c \ll 1$), which is valid for a highly swollen and dissolving polymer system, eq 2 reduces to

$$\frac{1}{T_2} = \frac{3}{2}\gamma^4\hbar^2\sum_k r_{jk}^{-6}\tau_c \qquad (3)$$

Equation 2 gives the form of the dipolar relaxation function in a highly mobile polymeric system, where the molecular mobility is considered as random isotropic reorientations of the H–H vectors. While it can be argued that such a simple treatment is seldom obeyed in a real polymeric system, eq 2 is adequate to provide a rationale for the interpretation of the NMR line width data based on the model we propose.

Equation 3 shows that the line width in the highly mobile phase is governed by τ_c. For polymers in solution, τ_c is typically 2–3 orders of magnitude longer than the value observed for low molecular weight liquids and one gets a line width of 10–30 Hz.

The foregoing discussion shows that one can directly use the observed proton line width as an internal mobility indicator to probe the swelling and the dissolution processes at the molecular level. The access to average mobility (m_{av}) in the system will be assumed to be given through the following approximate relationship.

$$m_{av} \propto T_2 \propto \frac{1}{\text{line width}} \qquad (4)$$

Experimental Section

Only some preliminary experiments have been conducted in this work to establish the use of *in situ* NMR measurements for probing the general features of dynamics of mobilization. A polyisoprene sample (molecular weight = 5.62×10^5) was used for the experimental studies. This was obtained in the form of a sheet of thickness 2 mm. The samples were cut into required sizes (4.7 × 4.7 × 2 mm) and taken for NMR measurement. The solvent used was $CDCl_3$, chosen to give a solvent-free spectrum and also satisfy the requirement for field-frequency lock. The cross-linked polymer was prepared by sulfur milling. The cross-linker used was limited to 2% by weight.

The NMR measurements were carried out on a Bruker MSL-300 FT-NMR spectrometer operating at the Larmor frequency of 300 MHz for protons in a conventional high-resolution 10-mm probe. The polymer sample was positioned at the center of the receiver coil with the help of a concentric 5-mm NMR tube containing approximately 0.5 mL of $CDCl_3$. The 5-mm tube containing $CDCl_3$ was positioned a little above the center of the receiver coil with the help of tight-fitting Teflon rings. The shim settings were adjusted with this setup with 2.5 mL of $CDCl_3$ in the 10-mm tube. Care was taken to collect the data immediately after positioning the sample piece of polyisoprene in the solvent. A typical lag was approximately 1–2 min, which was insignificant in comparison to the total duration of the experiment, which was usually of the order of 12 h.

The NMR experiments with agitation were carried out in a 10-mm NMR tube of approximately 6.5-cm length. A glass rod of 5-mm o.d. with a spindle at one end was used as the stirrer. The stirrer was properly positioned in the 5-mm rotor and loaded from the top. The sample was kept in the short 10-mm NMR tube which was placed in the conventional 10-mm high-resolution probe. The fids (free induction decays) were collected continuously in automation. It was convenient to measure the line widths directly from the spectra. Figure 1 depicts a typical set of absolute intensity data of the olefinic proton signal as a function of time. The line narrowing with time is indicative of the enhancement of internal mobility with time.

A macroscopic swelling measurement for cross-linked polymer was carried out at 21 °C. The ratio of the final to the original weight of the polymer is defined as the swelling ratio. This was directly plotted as a function of time.

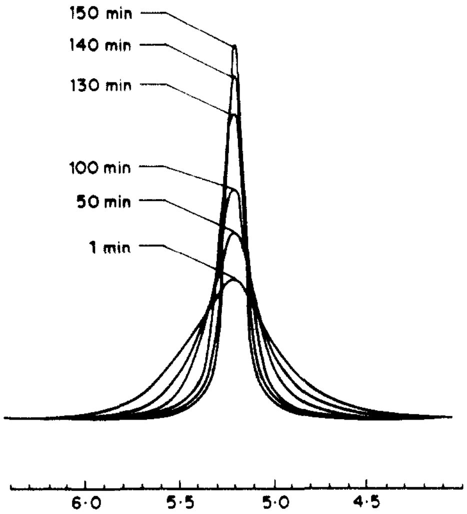

Figure 1. Variation of the olefinic proton signal of polyisoprene with time (in minutes). The spectra have been plotted in the absolute intensity mode. Typically 24 transients were accumulated in the time domain. A Lorentzian broadening of 5 Hz was used before Fourier transformation. Line width was measured at half intensity of these spectra.

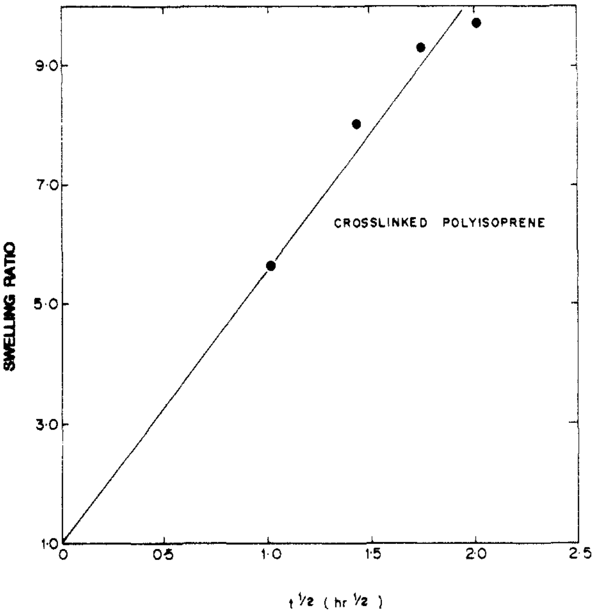

Figure 2. Plot of swelling ratio versus $t^{1/2}$ for partially cross-linked polyisoprene in $CDCl_3$.

Results and Discussion

Experimental Observations. Figure 2 shows the plot of the swelling ratio versus time for the cross-linked polymer. The dependence of the swelling ratio on square root of time is obvious. The corresponding response in the NMR experiment is shown in Figure 3a, where the line width of the olefinic proton could be accurately measured because of its chemical shift resolution. The line width of this proton resonance in polyisoprene in the absence of the solvent is 370 Hz. The reduced value of the line width of the polyisoprene is due to the considerable motional flexibility in this elastomeric solid. Upon addition of the solvent, there is a rapid decrease in line width (170 Hz after 2 min). Thereafter, the decrease is gradual. Interestingly, the plateau is sustained for an unusually long time interval, which lasts for about 50–60 min. Beyond this time, the line width again gradually decreases to a value of 32 Hz after 11 h.

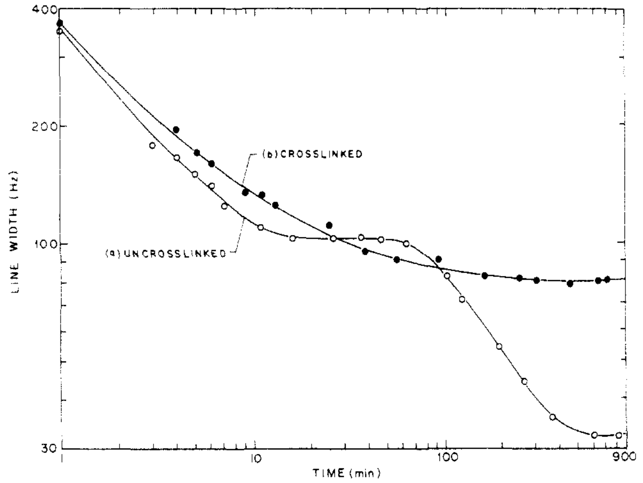

Figure 3. Variation of experimentally determined olefinic proton line width (Hz) with time for (a) un-cross-linked and (b) partially cross-linked polyisoprene under stagnant conditions.

The line width behavior in chemically cross-linked polyisoprene, on the other hand, is distinctly different (Figure 3b). There is an initial rapid decrease followed by a gradual change to a limiting line width of 80 Hz.

The presence of an intermediate plateau in the line width plot may be at first sight somewhat unexpected. The diffusion of solvent molecule seems to lead to an equilibrium swollen state, as judged from the microscopic NMR response in approximately the same time scale. Initially, the solvent diffusion is capable of segmental motion, which enhances the local mobility. This leads to a progressive decrease in the observed line width. In view of similar values of line widths, as expected in this polymer, the motional correlation times that lead to the observation of an equilibrium swollen state are of the same order as in the cross-linked polymer. While in the cross-linked polymer, the solvent-induced stress field is incapable of breaking the cross-links, the same field is sufficient to break the physical entanglements in the un-cross-linked polymer. That sufficient level of stress field has to be built up before this can happen is clear from the initial plateau that we have observed in this work. The concomitant opening up of chains and their interaction with the solvent lead to a complete dissolution of the polymer. This must, of course, occur by disentanglements of the associated networks.

Influence of Hydrodynamics. We investigated the effect of hydrodynamics on the swelling–dissolving polymer system. We obtained data by rotating the stirrer at 600 rpm. These data, presented in Figure 4, are compared with the data in the absence of a hydrodynamic field (stagnant conditions) for an un-cross-linked polymer. We observe interestingly enough that the first plateau now disappears altogether. In fact, the line width data only show a gradual decrease leading to a limiting value, which corresponds to the line widths that are typical of a polymer solution.

In order to understand the above interesting experimental observations clearly, an insight into the swelling–dissolution phenomena in an un-cross-linked polymer and the role of hydrodynamic shear is essential. We attempt this in the next section along with a preliminary mathematical model.

Mechanistic Events in the Swelling–Dissolution Process. Although the macroscopic issues connected with swelling and subsequent dissolution of polymers have been addressed for some time,[1] some of the key mechanistic details of this process are beginning to be addressed only

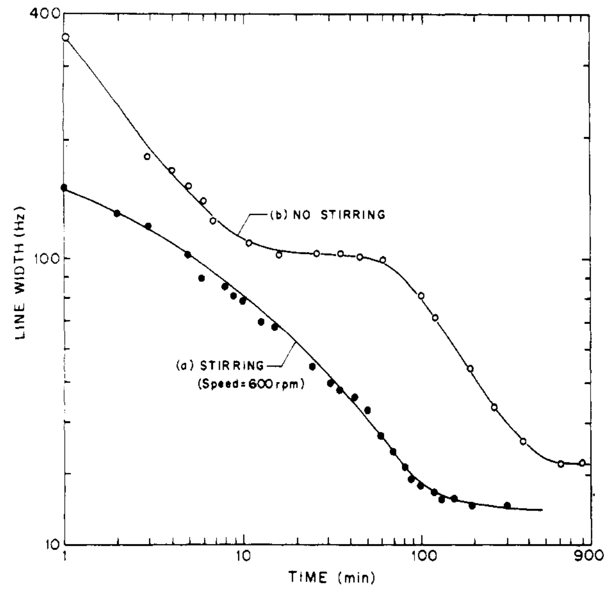

Figure 4. Variation of experimentally determined olefinic proton line width (Hz) with time under (a) stirred (600 rpm) and (b) stagnant conditions.

recently. In an important paper, Brochard and de Gennes[18] discussed the kinetics of dissolution of a droplet of polymer solution immersed in a pure solvent. The dissolution of these networks from the swollen state was shown to be governed by the rate of relaxation of the stress. This rate was estimated to be of the order of the reptation disengagement time. The dissolution of the polymer drop was shown to be crucially linked to the viscous yield phase.

Herman and Edwards,[19] in yet another significant paper, developed a model for swelling and dissolution of polymers in a good solvent based on the reptation theory. They analyzed the contribution to the free energy and the chemical potential of the polymer and the solvent due to the nonrandom distribution of orientations induced by the penetration of the solvent and the subsequent swelling. They concluded that when the contribution due to the nonrandom distribution of orientations is sufficiently large compared to the contribution arising from the spatial variation in the concentration, the system undergoes a phase separation into a gel-like concentration solution phase and a dilute solution phase. The viscous yield phase as described by Brochard and de Gennes[18] was suggested to be responsible for the dissolution of the gel-like phase.

We postulate that the process of dissolution of a rubbery polymer may comprise two distinct processes occurring concurrently, viz., swelling and disentanglement of the polymer chains. The process of swelling involves the ingress of the solvent molecules into the polymer, which is driven by the chemical potential difference between the bulk and the polymer matrix. As more solvent penetrates into the polymer matrix, the free volume available within the matrix increases and consequently both the segmental mobility of the polymer chain and the diffusion coefficient of the solvent increase. The solvent then penetrates at a faster rate, thus increasing the mobility of the chains even further. As the polymer volume fraction in the swollen polymer decreases, a stage is reached when the polymer chains acquire adequate mobility to break free from the entangled network. The motion of the chains during this stage may be due to reptation and/or other modes of motion characteristic of concentrated polymer solutions.[20] Such a mobile polymer chain on leaving the polymeric matrix will attain even higher mobility in the bulk solution.

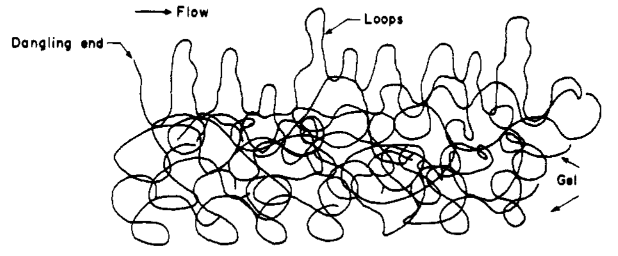

Figure 5. Disengagement model with dangling ends and loops of the polymer segments at the surface of the swollen gel.

The mechanistic details of this process of disentanglement have not yet been developed adequately.[21] The rate at which polymer chains leave the polymeric matrix at the polymer–liquid interface cannot be quantified in an *a priori* way. As an approximation, we assume an overall rate of dissolution R and on the basis of the experimental evidence available, this rate R will be assumed to be constant.[1,22] It is worth noting that while the glassy polymers show an induction period, the rubbery polymers do not. Hence, this constant rate will be assumed to apply at all times in the rubbery polymers.

Exact quantification of R is perhaps the most difficult problem to tackle. For low molecular weight solids, the dissolution process governing R has been envisaged[22–25] as one that involves two steps: detachment of atoms, molecules, or ions from the solid surface, followed by the diffusion of such species through an external mass transfer film into the bulk liquid. The driving force for the detachment is the thermodynamic solubility of the solid in the liquid. While this approach is reasonable for low molecular weight solutes, it is not applicable to polymer chains for two simple reasons. First, a "thermodynamic solubility" cannot be defined for polymers in a manner analogous to low molecular weight systems. Second, the polymer chains, being long and mutually entangled, are inhibited from entering the liquid phase due to the dynamic friction between the chains. The rate at which the chains disentangle becomes one of the factors controlling the dissolution rate. Indeed, the "disengagement" of the chain from the surface due to a hydrodynamic shear on the dangling ends of the polymer chains as well as the intermediate segments of the molecules as loops at the polymer–liquid interface constitutes an important step (see Figure 5). If the hydrodynamic force happens to be strong enough to release the polymer chains from entanglements, then it will greatly aid the dissolution process.

There is some support for the disengagement process postulated here when one looks at the distantly related problem of adsorption layers in polymer solutions.[26–30] Consider the work on ellipsometry studies of adsorbed polymer chains subjected to flow presented by Lee and Fuller.[26] These authors adsorbed the polymer chains under no-flow conditions and then subjected the chains to the flow of the bulk liquid above the surface. For a weakly adsorbed high molecular weight flexible chain, only a small proportion of the polymer segment is actually attached to the surface, with the remainder extending away from the surface as dangling ends or loose loops. They observe that "imposition of hydrodynamic forces can result in distortion and alignment of those unattached segments. Furthermore, if the shear stress is large enough, it is conceivable that the chains could be torn away from the surface", and this is directly relevant in the context of our model.

There is also some more indirect evidence[31] for our postulate of disengagement of dangling chains under hydrodynamic forces. For example, rheological studies of polymer solutions have shown an anomalous behavior due to the formation of a gel-like layer at the surface of the viscometers. An interesting study[31] of topological adsorption entanglement layer formation in high molecular weight polymers incorporates the mutual entanglement of the flowing solutions and that of the adsorbed layer along the surface. It is obvious that these entangled molecules at the surface will be torn away by increasing shear stress.

The next question to be addressed is as to whether the two processes of swelling and dissolution can be decoupled. At least a minimum swelling of a few layers of polymers chains at the surface of a rubbery polymer is required for the polymer chains to gain sufficient mobility to break out from the surface. Admittedly, beyond this minimum swelling, the role of the solvent in the disengagement of chains is not very well understood. We will decouple the two processes by assuming a constant rate of dissolution (R) that is independent of the swelling process. This will, of course, be true if the polymer volume fraction in the surface layers of the polymer matrix ($\phi_{p,i}$) is always lower that the critical polymer volume fraction required for the disengagement of the chains.

With this mechanistic background, we develop a preliminary mathematical model.

Model Development and Predictions. We set up a model for a one-dimensional system. As per convention,[19] we assume the mutual diffusion coefficient (D_m) at a polymer volume fraction (ϕ_p) is given by

$$D_m = D_0 \exp[\beta(1 - \phi_p)] \tag{5}$$

Here, D_0 is the solvent diffusion coefficient in the pure polymer (i.e., at $\phi_p = 1$) and β is a constant. The constant dissolution rate is defined as the rate (R) at which the swollen polymer reduces in size due to the polymer chains leaving the surface and will be measured in units of velocity. We further assume that the bulk volume is so large that the polymer concentration in the bulk solution is negligible, implying that the perfect sink conditions hold. Also as assumed earlier,[19] the surface of the polymer will be assumed to attain a constant concentration equal to $\phi_{p,i}$, immediately after contact with the solvent. In a nondissolving polymer (like a cross-linked polymer), $\phi_{p,i}$ will decide the equilibrium swollen length of the polymer matrix.

The mass balance equations for ϕ_p can be written as[32]

$$\frac{\partial \phi_p}{\partial t} = \frac{\partial}{\partial x}\left(D_m \frac{\partial \phi_p}{\partial x}\right) \tag{6}$$

where the volume fractions ϕ_p and ϕ_s are related as follows:

$$\phi_p + \phi_s = 1 \tag{7}$$

The initial and boundary conditions are as follows:

$$\phi_p = 1 \quad \text{at } t = 0;\ 0 < x < L_0 \tag{8}$$

$$\phi_p = \phi_{p,i} \quad \text{at } x = l(t);\ t > 0 \tag{9}$$

$$\partial\phi_p/\partial x = 0 \quad \text{at } x = 0;\ t > 0 \tag{10}$$

Here, L_0 is the initial half-length of the polymer slab and $l(t)$ is the half-length at time t.

The boundary of the polymer slab, as defined by $x = l(t)$, moves at a rate given by

$$\frac{dl}{dt}\phi_{p,i} = \left[D_m \frac{\partial \phi_p}{\partial x}\right]_{x=l} - R\phi_{p,i} \tag{11}$$

In eq 11, the first term on the right-hand side represents the increase in length of the slab due to swelling caused by solvent influx, whereas the second term denotes the rate of decrease of the length due to the disengagement of the polymer chains from the surface. Obviously, we have

$$l = L_0 \quad \text{at } t = 0 \tag{12}$$

Here, L_0 is initial half-length of the polymer particle. The above equations can be made dimensionless by defining a dimensionless time ($\theta = D_0 t/L_0^2$), a dimensionless distance ($\xi = x/L_0$), and a dimensionless length ($L = l(t)/L_0$).

The solution of the equations will give us the concentration profiles. We used the Crank–Nicolson finite difference method to obtain this profile. The next task now is to relate the information on concentration profiles, and in turn on $\phi_s(\theta,\xi)$, to the local mobility and the average mobility.

Mobility in a Swelling–Dissolving Polymer. As the polymer swells, the free volume of the swollen polymer network increases. As the polymer dissolves, the mobility of the molecules in the solvent phase further increases due to the higher free volume available in the solvent phase. Following the conventional free volume model,[33] the mobility of the molecules in the gel phase may be expressed as follows:

$$m_g = A_d \exp(-B_d/f_g) \tag{13}$$

Here, m_g is the mobility of the molecules in the gel phase, B_d and A_d are constants which depend on the size and shape of the molecules, and f_g is the fractional free volume of the gel phase. The fractional free volume of the gel phase can be calculated by using the usual additivity relationship.[33]

$$f_g = f_p\phi_p + f_s(1 - \phi_p) \tag{14}$$

Here, f_s is the free volume fraction of the solvent and f_p is the free volume fraction of the polymer.

The mobility of the molecules in the solvent phase may be also expressed similarly as follows.

$$m_s = A_d \exp(-B_d/f_s) \tag{15}$$

where m_s is the mobility of the molecules in the solvent phase and f_s is the free volume in the solvent phase.

In our case, the mobility measured is a value averaged over the number of polymer chains enjoying the same free volume. Hence, we define an average mobility as

$$m_{av} = \frac{1}{L}\int_0^1 \phi_p m_g \, d\xi + \left(\frac{\phi_{p,i}Rt}{L_0}\right)m_s \tag{16}$$

To limit the value of m_{av} between 0 and 1, we also define a normalized average mobility.

$$\langle m_{av}\rangle = \frac{\int_0^L \phi_p m_g \, d\xi}{L m_s} + \left(\frac{\phi_{p,i}Rt}{L_0}\right) \tag{17}$$

Note that while the first term on the right-hand side represents the contribution to the overall mobility by the chains with polymer (say $\langle m_{av}\rangle_g$), the second term is the contribution of the polymer chains in the bulk solution (say $\langle m_{av}\rangle_s$). For a very high R or at large times, the contribution to the average mobility of the polymer chains in the bulk will be large compared to the contribution of the swollen polymer. The experimental measurements done in this paper relate to the NMR line width. Equations 4 and 17 couple these two together.

The dynamics of mobilization can be studied by examining the variation of the average mobility with time. The results of simulation for various values of the dimensionless parameter $\mu = RL_0/D_0$ are shown in Figure

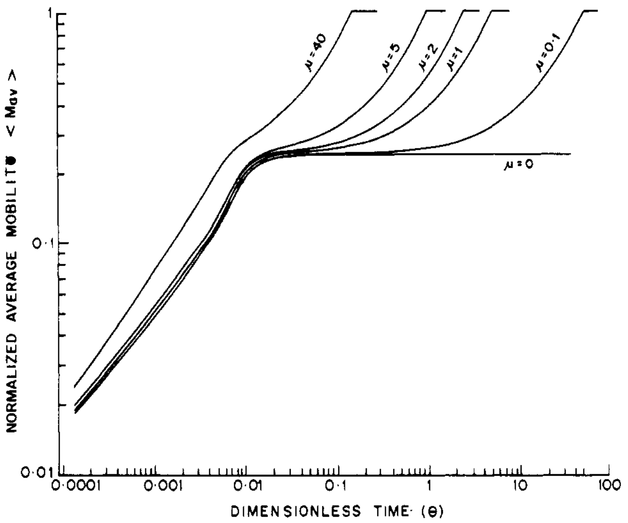

Figure 6. Effect of the parameter μ on the variation of the average mobility with dimensionless time (B_d = 3.0, β = 9.5, $\phi_{p,i}$ = 0.2).

6. Interestingly, the mobility–time plots for the system exhibit a double plateau for low values of μ, i.e., slow dissolution rates, whereas for higher values of μ (brought out physically by higher rates of detachment through the imposition of a hydrodynamic field) the early plateau disappears.

The occurrence of a double plateau can be explained on physical grounds. At small times, the polymer chains within the matrix gain mobility due to the solvent ingress. If the dissolution rate (R) is low, the number of chains in the bulk solution is very low. Hence, $\langle m_{av}\rangle_s$ is very small in comparison to $\langle m_{av}\rangle_g$. Therefore the mobility curve closely follows the trend of the fully cross-linked nondissolving system (μ = 0). If even at equilibrium swelling $\langle m_{av}\rangle_s$ is low compared to $\langle m_{av}\rangle_g$, then the early plateau corresponding to equilibrium swelling is seen. Subsequently, at some large times, the number of chains in the bulk solution increases so that the contribution of $\langle m_{av}\rangle_s$ becomes larger than the contribution of $\langle m_{av}\rangle_g$. Hence, an increase in mobility is seen, which finally terminates in a second plateau corresponding to the disappearance of the polymer matrix, and at this point the dissolution process is complete. This is further clear when we examine the contribution of the gel phase and the free polymer chain in the solvent phase to the average mobility. The high value of m_s in comparison to m_g plays an important role in the double plateau. However, in stirred systems, the value of R is high. Consequently, the number of polymer chains in the bulk solution is high. Hence, both the contributions $\langle m_{av}\rangle_g$ and $\langle m_{av}\rangle_s$ are comparable, thus leading to a single plateau.

Comparison of the Predictions with Experimental Data. We now compare the model predictions with the experimental results. We will try to calculate the values of as many parameters as possible in an *a priori* way. As regards the diffusivity values, quantitative predictions are possible through the model proposed by Vrentas and Duda.[34] All the model parameters of the Vrentas–Duda model are available for the polyisoprene–$CHCl_3$ system, and they were assumed to be valid for the polyisoprene–$CDCl_3$ system. We calculated D_0 and β in eq 4 by imposing an exponential fit on the mutual diffusivity calculated using the Vrentas and Duda equation at small concentrations of the solvent. D_0 and β for our system were estimated to be 1.65 × 10^{-7} cm^2/s and 9.5, respectively.

The other parameters required for the analysis are f_p, f_s, B_d, L_0, $\phi_{p,i}$, and R. f_p was estimated for this analysis by using the WLF equation.[35] For f_s, a more direct method, namely the Sugden group contribution method,[34] was used. B_d could not be estimated *a priori*, since adequate information in the literature to estimate this value is not available. $\phi_{p,i}$, which dictates the equilibrium solvent content of the polymer, can be assumed to be the same as that for the cross-linked polymer, since only a very small amount of cross-linking agent was used. R cannot be estimated *a priori*. However, an easy method to estimate R from the experimental line width data is possible. Since, we have assumed a constant rate of dissolution, we would expect the complete slab to disappear in a time to be given by

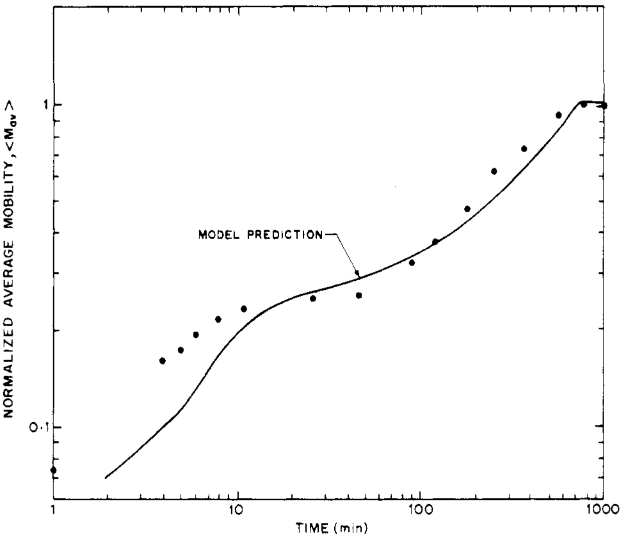

Figure 7. Comparison of the predicted normalized average mobility $\langle m_{av}\rangle$ with the normalized inverse line width of the olefinic proton under stagnant conditions. The experimental points are denoted by (●) while the continuous line represents the model prediction.

$$t_0 = \frac{L_0}{\phi_{p,i}R} \tag{18}$$

At time t_0, we will also expect the line width data to reach the second plateau. Hence, the line width data give us an estimate of t_0, thus giving us a value for R through eq 18. With these *a priori* estimations, the only remaining unknown parameter is B_d, which was treated as a curve fit parameter. The value used to obtain the best fit was B_d = 3. As can be seen from Figures 7 and 8, a reasonable semiqualitative agreement is seen to exist between the experimental line widths (represented here after inverting and normalizing) and the predicted normalized average mobility.

It is important to emphasize some of the limitations of our measurements. In the apparatus used by us, we can only probe the space-averaged mobility. It will be desirable to obtain the local mobilities in a small region. Our experiments would have been more meaningful if data on molecular weights below and above the critical molecular weight for entanglement were available, since it is expected that, below a critical molecular weight, the plateau should disappear. Unfortunately, such data have not been available due to want of samples with varying molecular weights of the same grade of polyisoprene. Future studies should be directed for such measurements.

It is also important to note some of the limitations of our analysis here. The model, formulated as a one-dimensional problem, is not strictly valid in the case of our experiments, since the polymer sample used by us was only approximately one-dimensional. Simultaneously,

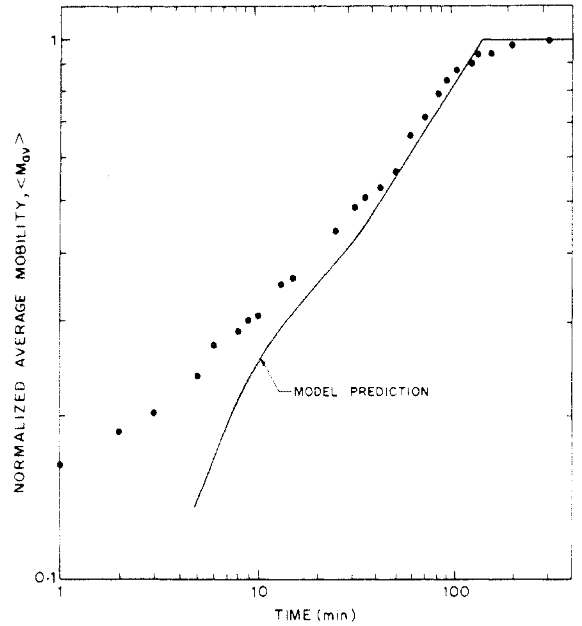

Figure 8. Comparison of the predicted normalized average mobility $\langle m_{av} \rangle$ with the normalized inverse line width of the olefinic proton under stirred conditions. The experimental points are denoted by (●) while the continuous line represents the model prediction.

parameters of the model such as $\phi_{p,i}$ and R cannot be quantified *a priori*, since the mechanistic details of the process have not yet been fully established. It is also necessary to note that the dissolution rate (R) combines the effects of several concurrent processes occurring in the swelling–dissolving polymer. Equation 4 is yet another important assumption which may have to be replaced by a more accurate expression. However, this will require further extensive studies.

In our attempt to explain the process of swelling–dissolution in polymeric systems, we also wish to raise some new questions. The line width vs time plot for uncross-linked polyisoprene indicates that the polymer takes around 10 min to swell to a "pseudoequilibrium swelling" at which it persists for at least 50 min before the overall mobility of the system increases due to an increase in the number of chains in the solvent phase. In the context of the recent models for polymer dissolution based on the reptation theory, such a persistent "pseudoequilibrium swelling" is unexpected. This observation requires further study both experimentally and theoretically, since it can give a vital insight into the mechanistic aspects of the process and also lead to a better understanding of the role of swelling in polymer dissolution. If the role of swelling is limited to providing a minimum mobility for the polymer chains to start disentanglement and if the dissolution rate is largely a surface phenomenon, then it will be possible to treat swelling and dissolution as essentially decoupled processes, as we have done in this work. This may largely simplify the analysis of swelling–dissolution phenomena in polymers, especially in systems such as used in this work, where the swelling was relatively fast. Another aspect requiring attention is the quantification of R, which will require a detailed microscopic modeling of the disentanglement and/or disengagement processes.

Conclusions

This study is a continuation of our sustained investigations into the dynamics of internal mobilization in superswelling polymeric systems[36-38] and use of this understanding for diffusion modulation in such systems.[39,40] This specific study of dynamics of mobilization of polymer molecules in a rubbery swelling–dissolving system brings out a number of new features. First, we have demonstrated that proton *in situ* NMR spectral measurements can be used to probe the dynamics in the swelling–dissolving systems at a microscopic level. The experimental line width data obtained can be explained at least semiquantitatively through a mathematical model developed by us.

The interesting new insight is that the dissolution phenomenon seems to be largely a surface phenomenon which may be decoupled from the swelling process. We venture to reach this conclusion since at the microscopic level, a minimum level of swelling, and therefore of internal mobilization, is required (as evidenced by NMR experiments) before the process of dissolution starts. We emphasize here that the role of solvent ingress in determining the dissolution rate seems to be limited to only allowing a minimum mobility to the polymer chains so that they can "break free". Polymer dissolution in a sheared medium has been postulated to be controlled by the "disengagement" of polymer chains at the polymer–liquid interface due to the action of hydrodynamic forces on the polymer chains dangling into the liquid.

Our experimental data clearly indicates the existence of a persistent "pseudoequilibrium swelling" of the polymer matrix, the reason for which is not very clear. A complete explanation for this will require a detailed study of the aspects of polymer disentanglement and disengagement.

References and Notes

(1) Ulberreiter, K. The Solution Process. In Crank, J., Park, G. S., Eds. *Diffusion in Polymers*; Academic Press: New York, 1968; Chapter VII.
(2) Crist, B. *J. Non-Cryst. Solid* **1991**, *131*–133, 709.
(3) Richter, D.; Fetters, L. J.; Huang, J. S.; Farago, B.; Ewen, B. *J. Non-Cryst. Solids* **1991**, *131–133*, 164.
(4) Pajevic, S.; Bansil, R.; Konank, C. *J. Non-Cryst. Solids* **1991**, *131–133*, 630.
(5) Davis, P. J.; Pinder, D. W.; Callaghan, P. T. *Macromolecules* **1992**, *25*, 170.
(6) Webb, A. G.; Hall, L. D. *Polym. Commun.* **1990**, *31*, 422.
(7) Webb, A. G.; Hall, L. D. *Polym. Commun.* **1990**, *31*, 425.
(8) Cohen-Addad, J. P.; Domard, M.; Herz, J. *J. Chem. Phys.* **1982**, *76*, 2744.
(9) Fukumori, K.; Kurauchi, T.; Kamigaito, O. *Polymer* **1990**, *31*, 713.
(10) Fukumori, K.; Kurauchi, T.; Kamigaito, O. *Polymer* **1990**, *31*, 2361.
(11) Abragam, A. *The Principles of Nuclear Magnetism*; Oxford University Press: London, 1961; Chapter IV.
(12) Slichter, C. P. *Principles of Magnetic Resonance*; Springer-Verlag: Berlin, 1990; Chapter III.
(13) Forbes, J.; Bowers, J.; Xi Shan; Morant, L.; Oldfiled, E.; Moscarello, M. A. *J. Chem. Soc.*, Faraday Trans. *1* **1988**, *84*, 3821.
(14) Ganapathy, S.; Badiger, M. V.; Rajamohanan, P. R.; Mashelkar, R. A. *Macromolecules* **1989**, *22*, 2023.
(15) Schneider, B.; Doskocilova, D.; Dybal, J. *Polymer* **1985**, *26*, 253.
(16) Forbes, J.; Husted, C.; Oldfield, E. *J. Am. Chem. Soc.* **1988**, *110*, 1059.
(17) Bloembergen, N.; Purcell, E. M.; Pound, R. V. *Phys. Rev.* **1948**, *73*, 679.
(18) Brochard, F.; de Gennes, P. G. *PhysicoChem. Hydrodyn.* **1983**, *4* (4), 313.
(19) Herman, M. F.; Edwards, S. F. *Macromolecules* **1990**, *15*, 3662.
(20) Fujita, H. *Polymer Solutions*; Elsevier Science Publishers, B. V.: Amsterdam, 1990.
(21) Yih-O, Tu; Ouano, A. C. *IBM J. Res. Dev.*, March 1977, 131.
(22) Lapcik, L.; Valko, L., *J. Polym. Sci.*, A2 **1971**, *9*, 633.
(23) Rosner, D. E. *J. Phys. Chem.* **1969**, *73*, 382.
(24) Cooney, D. O. *AIChE J.* **1972**, *18* (2), 446.
(25) Gallily, I.; Friedlander, S. K. *J. Chem. Phys.* **1965**, *42*, 1503.
(26) Lee, J.; Fuller, G. G. *Macromolecules* **1984**, *17*, 375.
(27) Hatano, A. *Polymer* **1984**, *25*, 1198.

(28) Lee, J.; Fuller, G. G. *J. Colloid Interface Sci.* **1985**, *107* (2), 308.
(29) Cohen, Y.; Metzner, A. B. *Macromolecules* **1982**, *15*, 1425.
(30) Cohen, Y. *Macromolecules* **1988**, *21*, 494.
(31) Barham, P. J.; Keller, A. *Macromolecules* **1990**, *23*, 303.
(32) Crank, J. *Mathematics of Diffusion*; Oxford University Press: London, 1975.
(33) Kulkarni, M. G.; Mashelkar, R. A. *Chem. Eng. Sci.* **1983**, *38* (6), 925.
(34) Zielinski, J. M.; Duda, J. L. *AIChE J.* **1992**, *38* (3), 405.
(35) Berry, G. C.; Fox, T. G. *Adv. Polym. Sci.* **1968**, *5*, 261.
(36) Badiger, M. V.; Kulkarni, M. G.; Rajamohanan, P. R.; Ganapathy, S.; Mashelkar, R. A. *Macromolecules* **1991**, *24*, 106.
(37) Rajamohanan, P. R.; Badiger, M. V.; Ganapathy, S.; Mashelkar, R. A. *Macromolecules* **1991**, *24*, 1423.
(38) Ganapathy, S.; Badiger, M. V.; Rajamohanan, P. R.; Mashelkar, R. A. *Macromolecules* **1992**, *25*, 4255.
(39) Badiger, M. V.; Kulkarni, M. G.; Mashelkar, R. A. *Chem. Eng. Sci.* **1992**, *47*, 3.
(40) Kulkarni, M. G.; Premnath, V.; Patil, S. S.; Mashelkar, R. A. *Proc. R. Soc. London* **1992**, *439*, 397.